

Liquid boron and amorphous boron: An ab initio molecular dynamics study



Murat Durandurdu

Department of Materials Science & Nanotechnology Engineering, Abdullah Gül University, Kayseri 38080, Turkey

ARTICLE INFO

Article history:

Received 23 January 2015

Received in revised form 24 February 2015

Accepted 8 March 2015

Available online 14 March 2015

Keywords:

Boron;

Amorphous;

Liquid;

B₁₂ icosahedra

ABSTRACT

The atomic structure of liquid and amorphous boron is investigated using an ab initio molecular dynamics technique. Liquid and amorphous states are found to have notably different microstructures and an average coordination number. Ideal and defective pentagonal pyramidal polyhedrons are the primary building unit of liquid boron but B₁₂ icosahedra do not exist in the liquid state. During the rapid solidification, more ideal pentagonal pyramids develop progressively, resulting into a gradual formation of B₁₂ icosahedra. On the basis of our findings, the atomic packing of pure amorphous boron is proposed to be somewhat close to that of the α -rhombohedral phase in contrast to the previous suggestions.

© 2015 Elsevier B.V. All rights reserved.

1. Introduction

Boron is one of the most fascinating and complex elements exhibiting different varieties of novel and unusual properties such as having many physical forms (called allotropes), neutron absorption, hardness, resistivity to heat, and changing bonding character by small impurities [1,2]. Considerable efforts have been made to understand pure boron but it still remains as a mystery element [3,4]. Because of its unique physical and mechanical properties, it has a wide range of technological applications [5–7].

Several different crystalline phases have been proposed for boron but so far experimental and theoretical studies revealed a few crystalline forms at ambient and high temperature and pressure conditions for pure boron. They are α -rhombohedral (B₁₂) [8], β -rhombohedral (B₁₀₆) [9], γ -orthorhombic (B₂₈) [10], tetragonal (B₁₉₂) [11], tetragonal (B₅₂) [12], α -Ga crystal structure (B₂) [10], and ϵ -rhombohedral (B₁₅, isostructural to boron carbide B₁₃C₂ if carbon atoms are substituted by boron ones) [13]. These crystalline polymorphous commonly have a very complex structure but all have one thing in common: their principal building blocks are dominated by the quasimolecular B₁₂ icosahedra.

In addition to the crystalline modifications, amorphous form of boron also exists and can be prepared using a variety of experimental techniques such as physical vapor deposition [14], chemical vapor deposition [15], pyrolysis [16], or rapid cooling [17]. The atomic packing of amorphous boron is believed to be similar to the crystalline phases, that is, the key local structural units are due to the randomly packed the B₁₂ icosahedra without a long-range order [18,19].

The short-range order of liquid boron remains unspecified as well because of some difficulties to handle it experimentally [20,21]. Liquid boron is indeed very reactive with any container and hence limited experimental investigations can be found in the literature. Regrettably the microstructure of liquid boron could not be unambiguously determined in these experiments but it was argued that its short-range structural arrangement is essentially similar to that of crystalline and amorphous phases [21]. To our knowledge only two theoretical investigations [20, 22] based upon ab initio molecular dynamics (MD) simulations were employed to uncover the microstructure of the liquid state. Both studies found that the B₁₂ icosahedrons do not persist in liquid boron but they reported a contradictory finding about the survival of pentagonal pyramids. Therefore additional reliable simulations are unquestionably desirable to clear the inconsistent predictions and to reveal the true atomic structure of the liquid state of this important element.

Here we perform ab initio MD simulations to systematically explore the atomistic arrangement of not only liquid boron but also amorphous boron. Our simulations provide substantial and novel information regarding their microstructures. Ideal and incomplete pentagonal pyramids are the central building unit of the liquid state. However, the B₁₂ icosahedra do not survive in it but they form gradually during the rapid solidification process. Amorphous boron is proposed to be locally similar with the α -rhombohedral phase.

2. Methodology

To investigate the atomic structure of the liquid boron and amorphous boron, we used the SIESTA ab initio code [23] within the frame of the density functional theory. The method adopts a localized linear combination of numerical atomic orbitals. Norm-conserving nonlocal

E-mail address: murat.durandurdu@agu.edu.tr

pseudopotential was generated by Troullier and Martins scheme [24]. To calculate the exchange correlation energy we used the generalized gradient approximation that implemented Becke gradient exchange functional [25] and Lee, Yang, and Parr correlation functional [26]. A double- ξ basis set was employed for the valence electrons. A real space grid equivalent to a cut-off of 120 Ry was adopted to compute the electron density, the local part of the pseudopotential, and the Hartree and the exchange–correlation potential. The MD simulations were done using the NPT (constant number of atoms, constant pressure, and constant temperature) ensemble. We had a supercell having 224 atoms and periodic boundary conditions. Only Γ point was applied for the Brillouin zone integration. The orthorhombic boron with the simulation box lengths $A = 10.108 \text{ \AA}$, $B = 11.24 \text{ \AA}$ and $C = 13.974 \text{ \AA}$ was melted at 4500 K for 10.0 ps. The liquid state was quickly cooled to 2500 K in 3.5 ps. At this temperature, the liquid state was thermalized for 20 ps and then it was gradually annealed to 300 K using the cooling rate of 0.05 K/fs. A time step of 1 fs was used. The total simulation time was more than 85.0 ps. Temperature was controlled using the velocity rescaling method. The volume of the supercell at zero pressure was equilibrated via the Parrinello Rahman technique [27] without allowing shear deformation. The final dimensions of the supercell at 300 K were $A = 10.278418 \text{ \AA}$, $B = 16.590147 \text{ \AA}$ and $C = 10.649009 \text{ \AA}$. The last 1000 MD steps of the liquid state were gathered for the structural analyses. During the cooling process, a few configurations around some specific temperatures were used for the analyses.

3. Results and discussion

In order to confirm that the simulation time is long enough to capture the dynamics of the liquid state at 2500 K, the mean square displacement (MSD) shown in Fig. 1 is studied for the last 1000 MD steps using the isaacs program [28]. The MSD is proportional to t^2 up to 75 fs, representing a ballistic motion. Beyond that point, it displays a linear behavior, specifying a diffuse state. The linear functioning of the MSD additionally implies a state of equilibrium. Fitting the diffusive part with a straight line and using the Einstein relation, $\langle (r(t) - r(0))^2 \rangle = 6tD$, the diffusion constant D is computed to be about $1.3 \times 10^{-4} \text{ cm}^2/\text{s}$.

The temperature dependence of pair distribution function (PDF) is presented in Fig. 2. The most noticeable change in the PDF is the sharpening of the peaks with decreasing temperature, demonstrating more order in the structure. On the other hand, the position of all peaks is found to be not too sensitive to temperature. The first, second and third peaks of the liquid phase at 2500 K are located at 1.75 \AA , 3.14 \AA and 4.65 \AA , respectively, which are in good agreement with the experimental results of 1.76(8) \AA , 3.15(6) \AA and 4.7 \AA found for the liquid boron at 2600 K (2400 K) (Ref. 21). At 300 K, that is, for amorphous boron, the first three peaks are placed at 1.78 \AA , 3.02 \AA and 4.54 \AA , respectively, which are again sensibly in accordance with the experimental values of 1.80 \AA , 2.93 \AA , and 4.38 \AA [29]. It can be seen that the

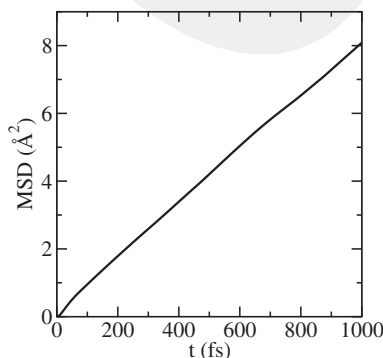


Fig. 1. The mean square displacement (MSD).

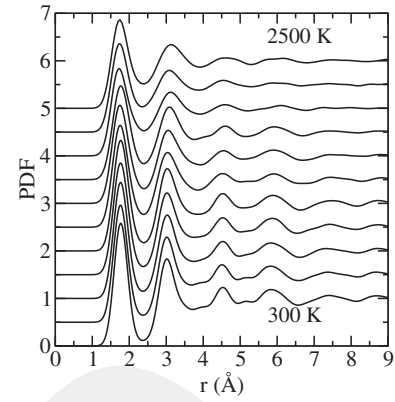


Fig. 2. Pair distribution function as a function of temperature.

model lacks long-range order since there is no clear peak beyond 7.0 \AA and the PDF approaches to one. Yet the slightly pronounced peaks around 3.0 \AA , 4.5 \AA and 6.0 \AA might be interpreted as the existence of medium-range order in the amorphous boron. A careful analysis suggests that the peaks start to be noticeable when B_{12} icosahedra form in the system near 1900 K and they become more pronounced as more ideal B_{12} icosahedra develop. Therefore it can be concluded that the medium-range order correlates with B_{12} icosahedra in the amorphous boron.

To have more complete information about the short-range order of liquid boron and amorphous boron, another critical parameter, average coordination number (CN), is studied as a function of temperature (Fig. 3). The CN gradually increases with decreasing temperature and reaches approximately a constant value of 6.1 around 1200 K. The CN of liquid boron at 2500 K is calculated to be 5.5, which is somehow lower than the experimental results of 5.8 ± 1 at 2600 K or 6.0 at 2400 K (Ref. 21) and the previous theoretical predictions of 6.0 [20, 22]. On the other hand, the CN of amorphous morphology at 300 K is 6.1, fairly close to the experimental value of 6.3 [29]. The distribution of CN is also evaluated and presented in Fig. 4. At 2500 K, the five- and sixfold coordinated atoms are dominated with a frequency of about 30%. With decreasing temperature, the fraction of sixfold coordination increases monotonically and touches the maximum value of about 65% around 1200 K. The parallel to the increase in the sixfold coordination, the fraction of fivefold and fourfold (12% at 2500 K) coordination declines during the solidification. Surprisingly, the sevenfold-coordinated atoms are found to be less responsive to temperature. About 16% and 15% of atoms are sevenfold coordinated at 2500 K and 300 K, respectively.

Voronoi polyhedral method [30] is used to further explore the structure at different temperatures. This technique is a practical approach to differentiate the short-range order in disordered systems. A Voronoi

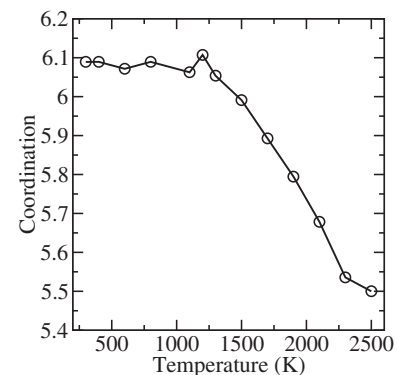


Fig. 3. Temperature dependence of coordination number (CN).

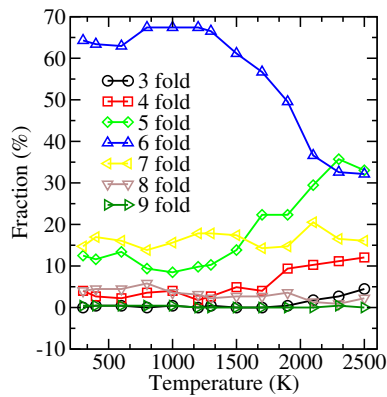


Fig. 4. Distribution of coordination number (CN) during rapid solidification.

polyhedron is characterized by indices $\langle n_3, n_4, n_5, n_6, \dots \rangle$. n_i gives the number of i -edge faces of polyhedron and 0 is the total CN. Fig. 5 shows the type and fraction of polyhedra. At 2500 K, a number of different types of polyhedrons are presented in the liquid state and the most prevalent ones are the $\langle 2, 3, 0, 0 \rangle$ and $\langle 2, 2, 2, 0 \rangle$ structures that are demonstrated in Fig. 6. Amorphous boron has almost the same type of clusters but the most favorable one is the $\langle 2, 2, 2, 0 \rangle$ polyhedron with a frequency of about 65%. The $\langle 2, 2, 2, 0 \rangle$ structures do indeed have the pentagonal pyramidal arrangement (see Fig. 6) whereas the $\langle 2, 3, 0, 0 \rangle$ cluster can be classified as an incomplete or defective pentagonal pyramid. The $\langle 2, 2, 2, 1 \rangle$ clusters are related to the pentagonal pyramid as well. The other sevenfold coordinated clusters also correlate with the $\langle 2, 2, 2, 1 \rangle$ polyhedron and can be categorized as a deformed/distorted $\langle 2, 2, 2, 1 \rangle$ type configuration. The $\langle 4, 0, 0, 0 \rangle$ arrangement is an unfinished pentagonal pyramid too. The $\langle 0, 6, 0, 0 \rangle$ formation is an incomplete $\langle 2, 2, 2, 1 \rangle$ polyhedron. Note that fivefold coordinated $\langle 2, 3, 0, 0 \rangle$ structure still persists in the amorphous model but its fraction is much less than that in the liquid state.

Although the pentagonal pyramidal type clusters exist in the liquid state, the quasimolecular B_{12} icosahedrons do not (Fig. 7). However, during the quenching process, complete B_{12} icosahedra are found to form between 2100 K and 1900 K and develop more as temperature is decreased. The computer generated amorphous boron model consists of B_{12} icosahedra, in good agreement with the experiments [18,19].

The arrangement of the B_{12} icosahedra in amorphous boron still remains a controversy. Experiments frequently suggested a local structure environment close to β -rhombohedral [31–33], although α -tetrahedral-like [34] or a transition state between α -rhombohedral and β -rhombohedral [19] was proposed for amorphous boron in

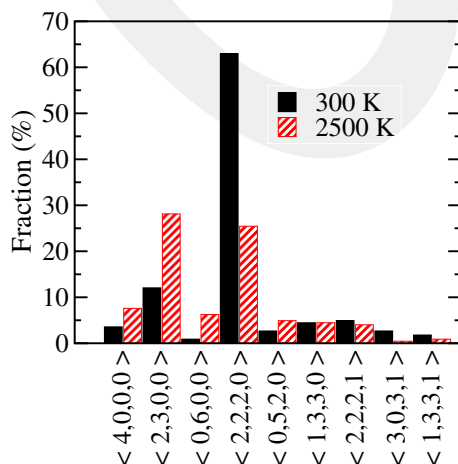


Fig. 5. Type and fraction of Voronoi polyhedrons.

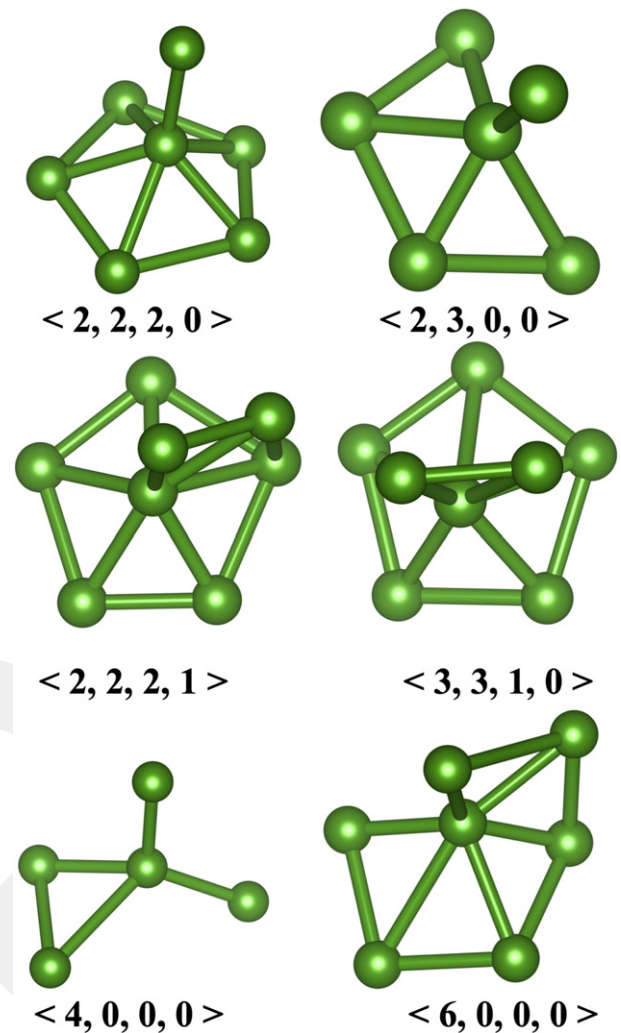
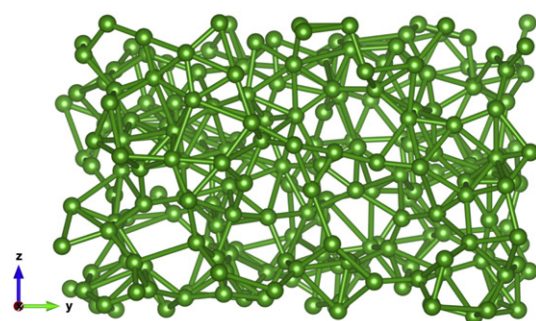


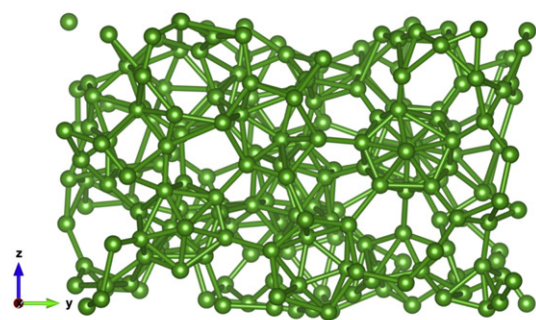
Fig. 6. Voronoi polyhedrons formed in the liquid boron and amorphous boron.

different investigations too. In order to recognize resemblances or distinctions of the computer generated amorphous model with these crystals, we carry out parallel investigations for them. β -Rhombohedral boron consists of B_{27} clusters having three B_{12} icosahedra sharing their faces. Such a B_{27} cluster does not exist in our model and thus it can be clearly eliminated from our consideration. α -Rhombohedral boron has dominantly $\langle 2, 2, 2, 0 \rangle$ and $\langle 2, 2, 2, 1 \rangle$ type polyhedrons. Note that neither tetragonal nor β -rhombohedral boron contains the $\langle 2, 2, 2, 1 \rangle$ cluster. Our amorphous model exhibits a small amount of $\langle 2, 2, 2, 1 \rangle$ configuration (about 15% including the defective ones), analogous to ones formed in the α -rhombohedral boron and hence it carries a signature of the α -rhombohedral phase. The tetragonal phase has two types of polyhedra $\langle 2, 2, 2, 0 \rangle$ and $\langle 4, 0, 0, 0 \rangle$ whose fraction is 94% and 4%, respectively. The $\langle 4, 0, 0, 0 \rangle$ type polyhedrons are also presented in the amorphous network but they are an incomplete pentagonal pyramid structure as discussed above and thus different from those formed in the tetragonal phase. Therefore, an important feature of the tetragonal phase is not offered in the amorphous model. Based on all these findings, we propose that the amorphous boron is partially similar to the α -rhombohedral crystal, which is however in conflict with the experiments [31–33].

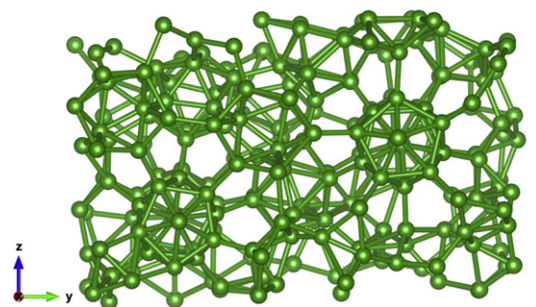
Several factors might be responsible for these distinct predictions. Perhaps the most important factor is the sample properties. In the simulations, the model is 100% pure in contrast to the samples used in experiments. Boron is indeed very sensitive to contaminations [4,21, 35,36] and depending on the concentration and content of impurities,



2500 K



1900 K



300 K

Fig. 7. Liquid boron, supercooled boron and amorphous boron.

it can have substantially dissimilar microstructures. Consequently, impurities might be the core reason for the contradictory observations for amorphous boron. The major limitations of simulations such as the time scale and the size of simulation box might be another important factor for having an amorphous topology, different than the experimental ones. Possibly the size of supercell is not big enough to capture B_{27} clusters or the cooling rate is too fast to see the formation of B_{27} clusters in the simulations.

On the basis of our interpretations of some experiments, however, we believe that amorphous boron locally related to the α -rhombohedral modification actually exists and our computer-generated amorphous network fairly describes the atomic structure of 100% pure amorphous boron in spite of some limitation mentioned above. Our first argument is the crystallization of amorphous boron [12,33,35–37]. The sequence amorphous \rightarrow α -rhombohedral \rightarrow β -rhombohedral

phase transformations were observed in some experiments during the thermal treatment [35]. The amorphous \rightarrow α -rhombohedral phase transition usually occurred in the pyrolytic amorphous powders [35,36] that had very low impurity concentrations. When the different impurities with different weights were artificially introduced in the pyrolytic samples, the crystallization mechanism was easily changed and the amorphous to α -rhombohedral phase transformation was hindered [35]. On the other hand, in the electrolytic amorphous boron with higher impurity concentrations relative to pyrolytic amorphous boron, the crystallization into α -rhombohedral crystal was not observed and instead a direct transition into β -rhombohedral phase took place [35, 36]. Under the same thermal treatment conditions, the crystallization into different phases implies that the pyrolytic and electrolytic amorphous samples have obviously a distinct structural packing, probably close to the α -rhombohedral and β -rhombohedral modifications, respectively to exhibit such phase transformations since it does not make sense that a β -rhombohedral-like amorphous phase transforms first the α -rhombohedral phase and then transforms back to the β -rhombohedral crystal with increasing temperature.

Our second argument is the general tendency of most amorphous materials to attain a topology locally similar to their corresponding ground state crystalline counterpart. The ground state of boron was a long lasting debate: the β -rhombohedral crystal was believed to be the ground state since it was the most common phase uncovered in experiments. However recent experiment [3] finalized this debate and showed that the α -rhombohedral modification is indeed thermodynamically stable and the ground state of boron. Therefore, it is quite sensible to anticipate amorphous boron having the building blocks close to the α -rhombohedral state.

4. Conclusions

We have performed ab initio MD simulations to have the atomistic level description of liquid and amorphous boron. We have found that ideal and imperfect pentagonal pyramidal clusters are the major building unit of the liquid state and B_{12} icosahedra gradually develop during the solidification process. The atomic arrangement of the computer-generated pure amorphous model is found to be comparable with that of the α -rhombohedral crystal, in stark contrast to experiments. Further theoretical investigations are surely critical to understand the influences of different impurities having different concentrations on the atomic structure of liquid boron and amorphous boron, which will lead us to interpret the physical origin of the distinct observations regarding the structural arrangements of amorphous boron.

Acknowledgments

The author is grateful to Dr. Artem Oganov for the information about the crystalline boron phases. This work was supported by the Scientific and Technical Research Council of Turkey (TÜBİTAK) under BİDEB-2232 program and grant no: 114C100.

References

- [1] <http://www.chemistryexplained.com/elements/A-C/Boron.html>.
- [2] <http://www.chemicool.com/elements/boron.html>.
- [3] G. Parakhonskiy, N. Dubrovinskaya, E. Bykova, R. Wirth, I. Dubrovinsky, *Sci. Rep.* 1 (2011).
- [4] A.R. Oganov, V.L. Solozhenko, *J. Superhard Mater.* 31 (2009) 285.
- [5] R.F. Barth, J.A. Coderre, M.G.H. Vicente, T.E. Blue, *Clin. Cancer Res.* 11 (2005) 3987.
- [6] <http://www.etimineusa.com/en/applications>.
- [7] T. Abu-Hamed, J. Karni, M. Epstein, *Sol. Energy* 81 (2007) 93.
- [8] B.F. Decker, J.S. Kasper, *Acta Crystallogr.* 12 (1959) 503.
- [9] R.E. Hughes, C.H.L. Kennard, D.B. Sullenger, H.A. Weakliem, D.E. Sands, J.L. Hoard, *J. Am. Chem. Soc.* 85 (1963) 361.
- [10] A.R. Oganov, J. Chen, C. Gatti, Y. Ma, Y. Ma, C.W. Glass, Z. Liu, T. Yu, O.O. Kurakevych, V.L. Solozhenko, *Nature* 457 (2009) 863.
- [11] M. Vlasse, R. Naslain, J.S. Kasper, K. Ploog, *J. Solid State Chem.* 28 (1979) 289.
- [12] O.O. Kurakevych, Y. Le Godec, T. Hammouda, C. Goujon, *High Press. Res.* 32 (2012) 30.

- [13] Gleb Parakhonskiy, Synthesis and Investigation of Boron Phases at High Pressures and Temperatures(PhD thesis) Universität Bayreuth, 2012.
- [14] L. Vandenbulcke, G. Vuillard, J. Electrochem. Soc. 123 (1976) 278.
- [15] K. Shirai, S. Gonda, J. Appl. Phys. 6 (1990) 6286.
- [16] K. Nakamura, J. Electrochem. Soc. 131 (1984) 2691.
- [17] F. Galasso, R. Vaslet, J. Pinto, Appl. Phys. Lett. 8 (1966) 331.
- [18] K. Katada, Jpn. J. Appl. Phys. 5 (1966) 582.
- [19] A.R. Badzian, Mater. Res. Bull. 2 (1967) 987.
- [20] D.L. Price, A. Alatas, L. Hennet, N. Jakse, S. Krishnan, A. Pasturel, I. Pozdnyakova, M.L. Saboungi, A. Said, R. Scheunemann, W. Schirmacher, H. Sinn, Phys. Rev. B 79 (2009) 134201.
- [21] S. Krishnan, S. Ansell, J.J. Felten, K.J. Volin, D.L. Price, Phys. Rev. Lett. 81 (1998) 586.
- [22] N. Vast, S. Bernard, G. Zerah, Phys. Rev. B 52 (1995) 4123.
- [23] P. Ordejón, E. Artacho, J.M. Soler, Phys. Rev. B 53 (1996) 10441.
- [24] N. Troullier, J.M. Martins, Phys. Rev. B 43 (1991) 1993.
- [25] A.D. Becke, Phys. Rev. A 38 (1988) 3098.
- [26] C. Lee, W. Yang, R.G. Parr, Phys. Rev. B 37 (1988) 785.
- [27] M. Parrinello, A. Rahman, J. Appl. Phys. 52 (1981) 7182.
- [28] S. Le Roux, V. Petkov, J. Appl. Crystallogr. 43 (2010) 181.
- [29] R.G. Delaplane, T. Lundstrom, U. Dahlborg, W.S. Howells, in: D. Emin, T.L. Aselage, A.C. Switendick, B. Morosin, C.L. Beckel (Eds.), Boron-Rich Solids, AIP Conf. Proc., No. 231, AIP, New York, 1991, p. 241.
- [30] S.Y. Wang, M.J. Kramer, M. Xu, S. Wu, S.G. Hao, D.J. Sordelet, K.M. Ho, C.Z. Wang, Phys. Rev. B 79 (2009) 144205.
- [31] K. Masayoshi, J. Mater. Sci. 23 (1988) 4392.
- [32] R.G. Delaplane, U. Dahlborg, W.S. Howells, T. Lundström, J. Non-Cryst. Solids 106 (1988) 66.
- [33] J.S. Gillespie Jr., J. Am. Chem. Soc. 88 (1966) 2423.
- [34] Y.G. Poltavtsev, V.P. Zakkarov, V.M. Pozdnyakova, Sov. Phys. Crystallogr. 18 (1973) 270.
- [35] S.O. Shalamberidze, G.J. Kalandadze, D.E. Khulelidze, B.D. Tsursumia, J. Solid State Chem. 154 (2000) 199.
- [36] I.A. Bairamashvili, et al., Neorg. Mater. (ISSR) 20 (1984) 409.
- [37] T. Machaladze, M. Samkharadze, N. Kakhidze, M. Makhviladze, Open J. Inorg. Chem. 4 (2014) 18.